Basic Characteristics of Ball Motion in a Twisting Ball Display

Tomohiro Tanikawa, Makoto Omodani▲ and Yasusuke Takahashi▲

Department of Electro-Photo Optics, Faculty of Engineering, Tokai University, Kanagawa, Japan

Shuichi Maeda

Advanced Technology Research Laboratory, Oji Paper Company, Tokyo, Japan

An electrical twisting ball display is one of the most promising candidates for digital paper but ball behavior remains to be clarified. We carried out basic experiments into ball behavior using an enlarged scale model, with particular emphasis on the threshold for the initiation of ball rotation and the response time for ball rotation as a function of the electric field and ball size. We found that an enlarged scale model can be used to predict the threshold electric field of a practical twisting ball display. The response times of both our model and practical twisting ball display are dependent on the electric field and the radius of the ball. We also derived a motion equation that explains the experimental results well.

Journal of Imaging Science and Technology 46: 557–561 (2002)

Introduction

The amount of digital information accessed continues to increase; the rapid spread of the internet is clearly one of the major causes. We can choose soft copy or hard copy to access digital information. Generally speaking, hard copy offers ease of reading and simpler handling; soft copy offers the advantages of ease of digital processing and reuse. Digital paper[1] appears to be the ideal medium that combines the advantages of both hard copy and soft copy. Over the years, several groups have investigated various candidates for digital paper, including reflective liquid crystal systems, electrical twisting ball displays[2–5] and electrophoretic image displays.[6] This study focuses on the twisting ball display, which we believe to be a promising candidate technology.

The twisting ball display is a bi-stable display, which consists of a large number of 30–100 μm diameter balls dispersed in a dielectric liquid in a transparent polymer sheet as shown in Fig. 1. Each ball has two colors: one hemisphere is black, the other white. The black and white hemispheres have different electric charges. Two electrodes are placed on the front and back of the sheet. The electric charge on the electrodes determines which side of each microsphere rotates upward. For example, when the white side is negatively charged, a positive charge on the electrode will cause the white side to rotate upward. Then the patterns of black and white can create images.

The balls are also known to develop a monopole charge equal to the net charge on the ball. Upon application of an electric field, the balls move across their cavities and rotate. Upon reaching the wall of its cavity, the rotation of each ball is arrested and this is the basis of the bi-stability of the display.

In this article, we will report the experimental results for the ball rotation using enlarged models, and its theoretical study, with particular emphasis on the threshold and the response time, as a function of the electric field and the size of the ball.

Experiment

Ball behavior was observed using enlarged model balls that are 100 times larger than those anticipated to be used in practical display sheets. The experimental apparatus is shown in Fig. 2. A ball made of nylon whose surface is divided into two areas with different colors and electric charges, is placed between two electrodes and floated at the boundary between two dielectric liquids with different specific gravities (Exxon Isopar-G™:0.75 and 3M fluorocarbon PF-5052:1.70). DC voltage is set between the pair of electrodes, and the rotation of the ball is recorded using a video camera (SONY DCR-TRV10). The response time was defined as the time taken for a ball to rotate 180 degrees. These experiments were repeated using balls with diameters of 3.2, 4.0, 4.8 and 5.6 mm. The representative conditions of the ball in the experimental cell are shown in Fig. 3. Figures 3(a), (b) and (c) show the ball before, under and after rotation, respectively. These photographs were taken perpendicular to the transparent electrodes.

Original manuscript received April 4, 2001

▲ IS&T Member

Supplemental Materials—Figures 1, 2, 3 and 8 can be found in color on the IS&T website (www.imaging.org) for a period of no less than two years from the date of publication.

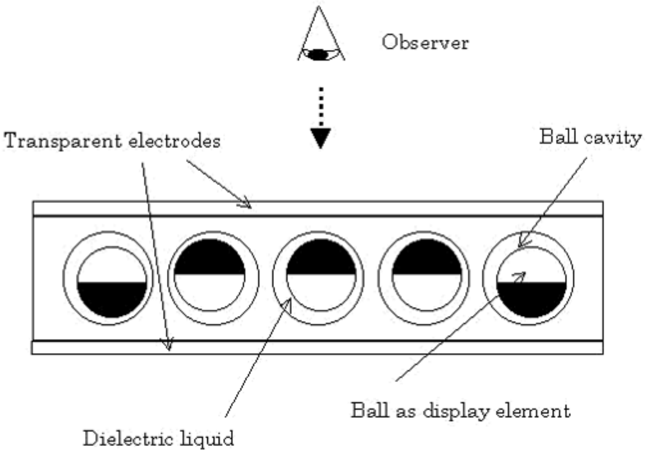

Figure 1. Schematic diagram showing twisting ball display. *Supplemental Materials can be found in color on the IS&T website (www.imaging.org) for a period of no less than two years from the date of publication.*

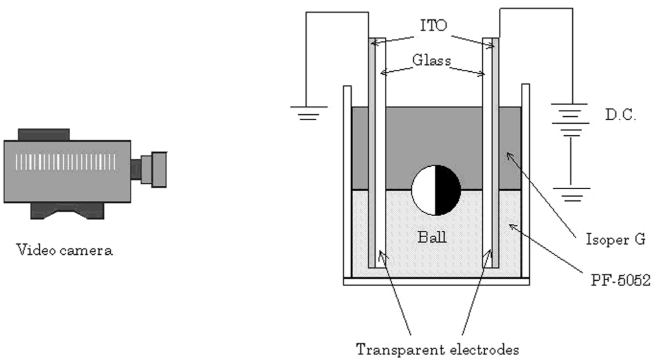

Figure 2. Experimental apparatus. *Supplemental Materials can be found in color on the IS&T website (www.imaging.org) for a period of no less than two years from the date of publication.*

Results and Discussion

Threshold Electric Field

There is a threshold for the initiation of ball rotation because the balls stick to their cavity wall in the case of the practical twisting ball display, and to the glass electrodes in the case of our experimental apparatus. Figure 4 shows the threshold electric field required for the rotation of balls with diameters of 3.2, 4.0, 4.8 and 5.6 mm (represented by the solid dots in the figure). These threshold electric fields tend to increase with ball diameter although the reason why a higher electric field is required with a larger ball is unclear at present. Presumably, however, the reason for this is related to the amount of surface electric charge, since the surface area relative to the volume of the ball increases as the ball size decreases. The higher surface electric charge relative to the ball volume has an advantage with respect to the driving moment for the ball rotation.

On the other hand, the threshold electric field of a practical twisting ball display with a 100 µm ball is calculated to be ca. 1300 V/cm using data from the literature.[5] The calculated data point (represented by the hollow dot) falls on the dashed line extrapolated from the experimental data in the figure. Therefore, it seems that our enlarged model can be used to predict the threshold at which rotation begins in a practical twisting ball display.

However, we think that confirming the correctness of this model requires consideration of other parameters.

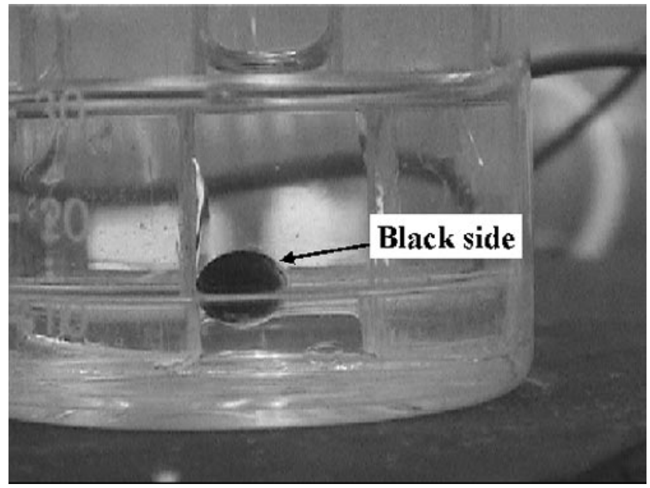

(a)

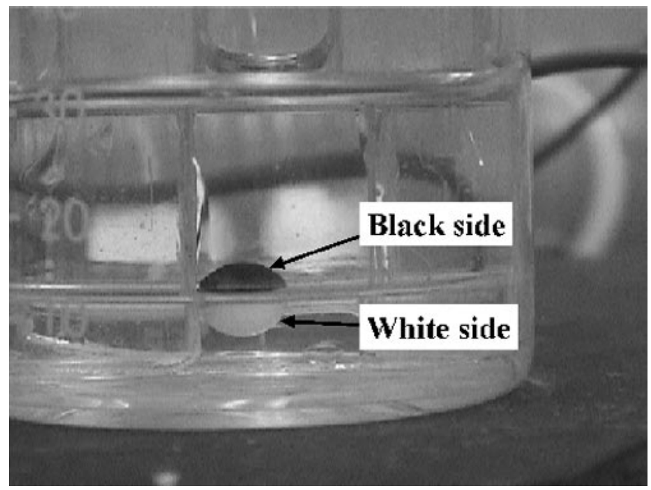

(b)

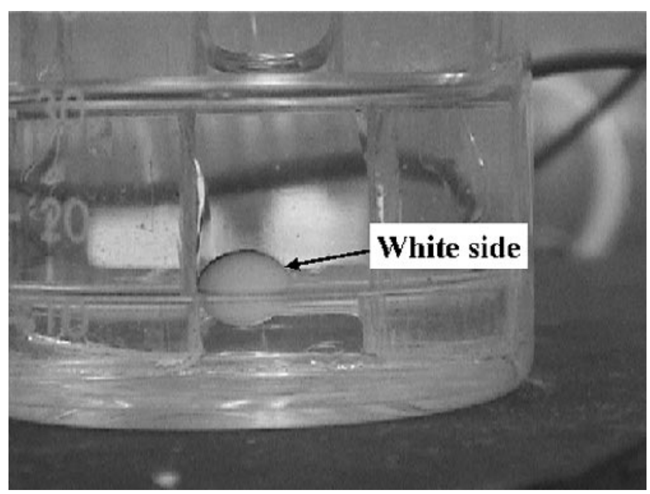

(c)

Figure 3. (a) Ball rotation in experimental cell (before rotation); (b) ball rotation in experimental cell (under rotation); and (c) ball rotation in experimental cell (after rotation). *Supplemental Materials can be found in color on the IS&T website (www.imaging.org) for a period of no less than two years from the date of publication.*

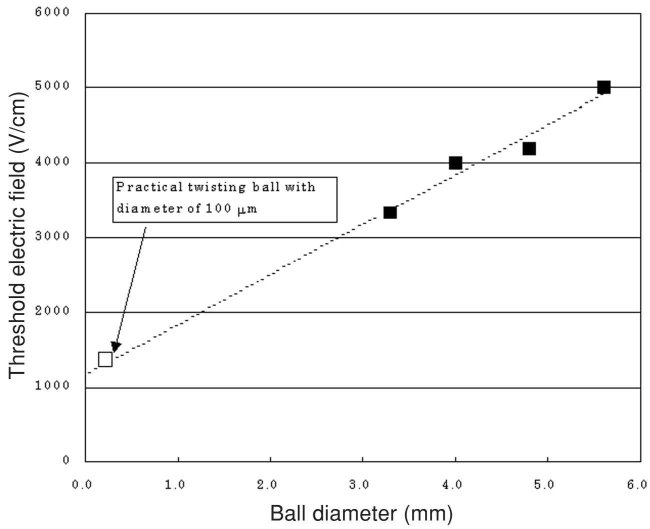

Figure 4. Threshold electric field required for the rotation of balls with diameter of 3.2, 4.0, 4.8, and 5.6 mm. The dashed line in Fig. 4 is a line of best fit through our experimental data points.

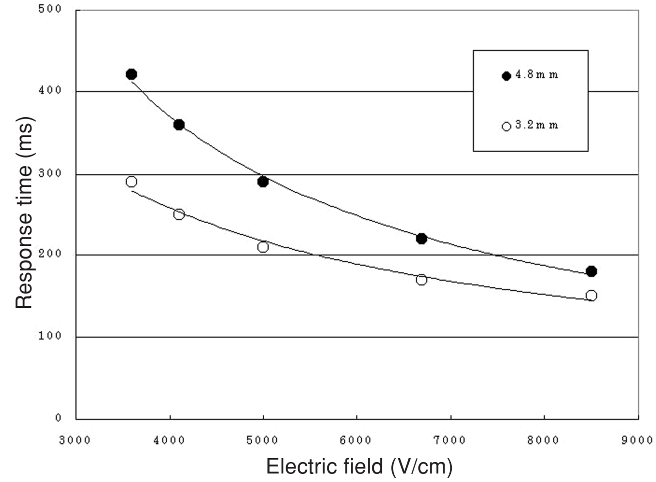

Figure 5. Response time curves as a function of electric field for enlarged model experiment.

This is because there are some differences between our experimental model and a practical twisting ball display. The physics of a practical twisting ball display was considered by Pham and co-workers[5] However, not all of this analysis applies to our experimental model, as well be discussed later.

According to Pham and co-workers,[5] in the case of practical twisting ball display, the sticking of the balls to their cavity walls is believed to have three causes, which will now be considered separately.

1) First of all, there is the van der Waals force that generally causes small objects to stick to one another. Van der Waals force is the attraction between oppositely charged ends of momentary, induced dipoles in neighboring molecules. These forces act between all molecules, even non-polar ones.
2) Secondly, the settling of a spherical ball into a soft spherical cavity constitutes a kind of hydraulic trap. As the ball is pulled into the wall by the monopole charge acted on by the electric field, the dielectric liquid is forced out and the wall distorts. So where the polymer which makes up the cavity is soft, there will be significant distortion of the wall by the ball.
3) The third force is believed to come from the electrical double layer at the interface between the ball surface and the dielectric liquid. The charge on the hemisphere of a ball is distributed over its surface and is just balanced by the total charge in the double layer, which consists of two regions: an inner region which may include adsorbed ions, and a diffuse region in which ions are distributed according to the influence of electrical forces and random thermal motion. As the ball nestles into the socket formed by the soft polymer, the dielectric liquid which is excluded carries an excess of oppositely charged ions, leaving the charged ball partially unshielded. This charge is then attracted to its image charge in the adjacent electrodes, pulling the ball into even tighter contact with the cavity wall.

In the case of our model, it seems that only the third of these forces applies. This is because, firstly, van der Waals forces have a very short range; they act only between the portions of different molecules which are in close contact, that is, between the surfaces of molecules. Secondly, our experimental apparatus does not have any cavities made of soft polymer that would produce a hydraulic trap.

Response Time

Figures 5 and 6 show the response time curves as a function of electric field for our experiment with 3.2 and 4.8 mm balls, and for a practical twisting ball display cited in literature,[5] respectively. Essentially the same relationships between the response time, electric field and ball size were observed both in our model experiment and for the practical twisting ball. The response time decreases as the electric field increases. Furthermore, the response time increases as ball size increases.

Theoretical Study of the Ball Rotation

A theoretical study was carried out in order to understand the experimental results of the ball rotation above. We looked at the rotation of a ball from its cross-section in order to simplify its behavior as shown in Fig. 7.

A Coulomb force is created when electric field, E, is applied, because the ball has an electric charge. The surface electric charge densities of the black and white regions are different (σ_b and σ_w, respectively). When the boundary between the black and white regions is θ degrees off the perpendicular to the electric field, a driving moment, M, is created and the ball starts to rotate because of the difference in electric charge density between the black and white regions. The rotation creates a dragging moment, m, because the dielectric liquid around the ball has viscosity, μ. Then the motion equation can be written as in Eq. (1), using the driving moment, large M, the dragging moment, small m, and the inertia moment, I.

$$M - m = I\, d^2\theta / dt^2 \tag{1}$$

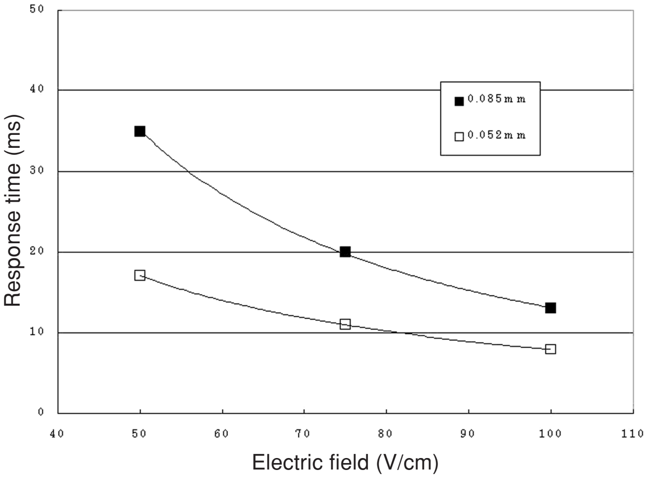

Figure 6. Response time curves as a function of electric field for practical twisting ball display (data from Ref. 5).

Let us start with the driving moment, M. Figure 8 shows a unit disk that has been sliced from the ball parallel to the electric field. It is being observed perpendicular to the field. Moments ΔM_b and ΔM_w are defined as unit moments at angular position α and $\alpha + \pi$, respectively. The moment of the unit disk, ΔM, is described by Eq. (2) using the Coulomb force, F, and electric charge, q.

$$\Delta M = \Delta M_b - \Delta M_w = F_b \sin\alpha = q_b E\, r \sin\alpha - q_w E\, r \sin\alpha \quad (2)$$

Considering q equal to σr, we can rewrite Eq. (2) as:

$$\Delta M = \sigma_b E r^2 \sin\alpha - \sigma_w E r^2 \sin\alpha = (\sigma_b - \sigma_w) E r^2 \sin\alpha \quad (3)$$

The term $(\sigma_b - \sigma_w)$ represents the difference in the surface electric charge densities of the black and white regions of the ball. When $\sigma_b - \sigma_w = \sigma$, the unit moment, ΔM, is finally described as:

$$\Delta M = \sigma E r^2 \sin\alpha \quad (4)$$

The effective moment on the disk is considered only within the following limited range of angles α:

$$\pi/2 - \theta \le \alpha \le \pi/2 + \theta \quad (5)$$

The total driving moment on the unit disk is written as:

$$M_{disc} = \int_{\frac{\pi}{2}-\theta}^{\frac{\pi}{2}+\theta} \sigma E r^2 \sin\alpha \, d\alpha \quad (6)$$

Figure 8 also shows a unit disk that has been sliced from the ball parallel to the electric field. It is being observed parallel to the field. The center plane of the disk is offset by the distance y forming the ball center. The radius of the disk, r, is given by the ball's radius, R, and coordinate, y, as follows: $r = (R^2 - y^2)^{1/2}$. The driving moment for the whole ball is written as:

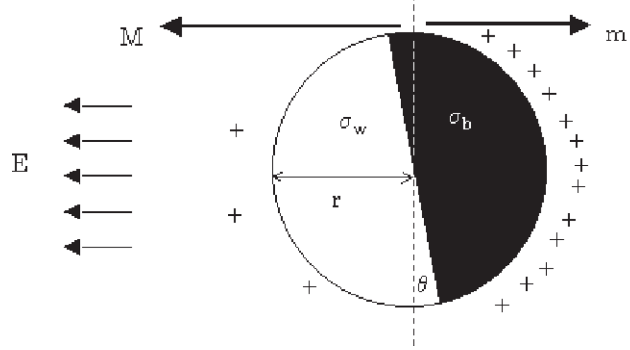

Figure 7. Cross sectional view of a ball.

$$M = \int_{-R}^{R} M_{disc}\, dy = 2\int_0^R \int_{\frac{\pi}{2}-\theta}^{\frac{\pi}{2}+\theta} \sigma E r^2 \sin\alpha \, d\alpha \, dy$$
$$= 2\int_0^R \int_{\frac{\pi}{2}-\theta}^{\frac{\pi}{2}+\theta} \sigma E \left(R^2 - y^2\right) \sin\alpha \, d\alpha \, dy \quad (7)$$

Equation (8) can be derived from Eq. (7):

$$M = (8/3)\sigma R^3 E \sin\theta \quad (8)$$

Moving our attention to the dragging moment of the ball, we write the dragging moment, m, as:

$$m = 8\pi\mu \, Rc^3 R^3/(Rc^3 - R^3)\, d\theta/dt \quad (9)$$

where Rc is the radius of a cavity sphere that has the same center as the ball. When the radius, Rc, is sufficiently large, Eq. (9) can be rewritten as:

$$m = 8\pi\mu \; R^3 \, d\theta/dt \quad (10)$$

We note that Eq. (9) and Eq. (10) were cited in *Hydrodynamics* by Lamb,[7] and the calculations were carried out in detail in that reference.

The inertia moment, I, of the ball is determined using the specific gravity of the ball, ρ, as[8]:

$$I = (8/15)\,\pi\,\rho R^5 \quad (11)$$

Using Eqs. (8), (10) and (11), we can rewrite Eq. (1) as:

$$(8/3)\,\sigma R^3 E \sin\theta - 8\pi\mu\, R^3\, d\theta/dt = (8/15)\pi\,\rho R^5\, d^2\theta/dt^2 \quad (12)$$

which can, in turn, can be rearranged as:

$$5\sigma E \sin\theta - 15\pi\mu\, d\theta/dt = (\pi\rho\, R^2)\, d^2\theta/dt^2 \quad (13)$$

This theoretical result suggests that the response time for ball rotation is dependent on the difference in surface charge densities between the black and white regions of the ball, σ, the electric field, E, the viscosity of the dielectric liquid, μ, the specific gravity of the ball, ρ, and the radius of the ball, R. The $5\sigma E\sin\theta$ term in Eq. (13), which correlates to the driving moment of the ball, becomes larger with higher electric field, E, while the $\pi\rho\, R^2$ term, which correlates to the inertia moment of

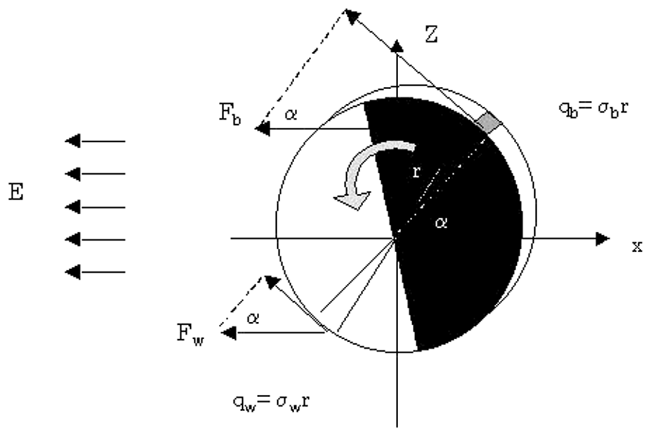

Figure 8. Rotation moment on the unit disk sliced from the ball parallel to the electric field, E. It is being observed perpendicular to the field. *Supplemental Materials can be found in color on the IS&T website (www.imaging.org) for a period of no less than two years from the date of publication.*

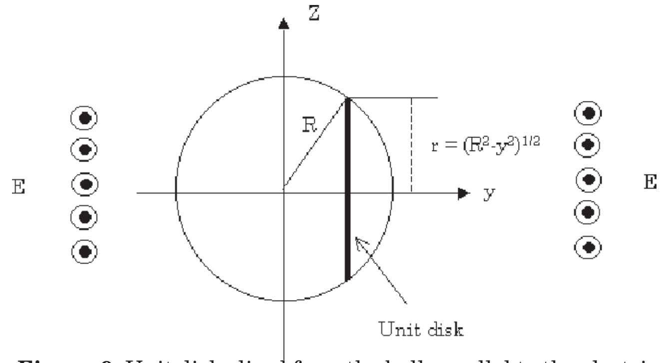

Figure 9. Unit disk sliced from the ball parallel to the electric field, E. It is being observed parallel to the field.

the ball, becomes smaller with smaller balls. The motion equation, Eq. (13), indicates that quicker response time in higher electric fields and with smaller balls results, at least in part, from the larger driving moment and the smaller inertia moment. This is an example that demonstrates good agreement between the theoretical study and the experimental results, although further consideration of the relationship between the theoretical study and the experimental results requires a solution of the differential equation, Eq. (13), is the next step in this study.

Conclusions

The threshold at which rotation begins and the rotation of the balls in an electric field were clarified experimentally using the enlarged scale model. We found that our enlarged scale model can be used to predict the threshold electric field of a practical twisting ball display, although further experimental work on other parameters is needed to confirm this model. The response time both of our model and the practical twisting ball display depend on the electric field, E, and on the radius of the ball, R. The motion equation derived from our theoretical study explains the experimental results quantitatively.

References

1. M. Omodani, *J. Image Soc. Jpn.* **38** 115 (1999).
2. N. K. Sheridon and M. A. Berkovitz, *Proc. SID* **18/3&4** 289 (1977).
3. N. K. Sheridon, *PPIC/JH'98* 83 (1998).
4. M. Saitoh, T. Mori, R. Ishikawa, and H. Tamura, *Proc. SID* **23**(4) 249 (1982).
5. T. Pham, N. Sheridon and R. Sprague, *SID'02 Digest,* 119 (2002).
6. B. Comiskey, J. D. Albert, H. Yoshizawa, and J. Jacobson, *Nature,* **394**(16), 253 (1998).
7. H. Lamb, *Hydrodynamics,* 6th ed., Cambridge University Press, Cambridge, UK, 1932 (from the Japanese translation by I. Imai, Tokyo Tosyo, 1988, p. 134).
8. A. Harashima, *Rikigaku,* 3rd ed., Shoukabou, Tokyo, Japan, 1992, p. 190.